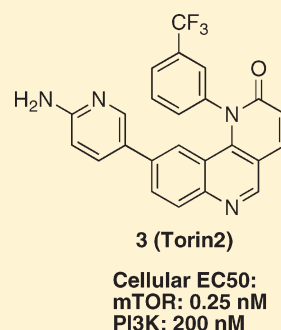


Discovery of 9-(6-Aminopyridin-3-yl)-1-(3-(trifluoromethyl)-phenyl)benzo[*h*][1,6]naphthyridin-2(1*H*)-one (Torin2) as a Potent, Selective, and Orally Available Mammalian Target of Rapamycin (mTOR) Inhibitor for Treatment of CancerQingsong Liu,<sup>†,‡</sup> Jinhua Wang,<sup>†,‡</sup> Seong A. Kang,<sup>§</sup> Carson C. Thoreen,<sup>†,‡</sup> Wooyoung Hur,<sup>†,‡</sup> Tausif Ahmed,<sup>||</sup> David M. Sabatini,<sup>§,⊥,‡</sup> and Nathanael S. Gray<sup>\*,†,‡</sup><sup>†</sup>Department of Cancer Biology, Dana Farber Cancer Institute, 44 Binney Street, Boston, Massachusetts 02115, United States<sup>‡</sup>Department of Biological Chemistry and Molecular Pharmacology, Harvard Medical School, 250 Longwood Avenue, Boston, Massachusetts 02115, United States<sup>§</sup>Whitehead Institute for Biomedical Research, 9 Cambridge Center, Cambridge, Massachusetts 02142, United States<sup>||</sup>Sai Advantium Pharma Ltd., 8-2-120/86/9/B "Luxor Park", Road No. 2, Banjara Hills, Hyderabad 500033, India<sup>⊥</sup>Department of Biology, Howard Hughes Medical Institute, Massachusetts Institute of Technology, Cambridge, Massachusetts 02139, United States<sup>\*</sup>Koch Center for Integrative Cancer Research at MIT, 77 Massachusetts Avenue, Cambridge, Massachusetts 02139, United States

## S Supporting Information

**ABSTRACT:** The mTOR mediated PI3K/AKT/mTOR signal transduction pathway has been demonstrated to play a key role in a broad spectrum of cancers. Starting from the mTOR selective inhibitor 1 (Torin1), a focused medicinal chemistry effort led to the discovery of an improved mTOR inhibitor 3 (Torin2), which possesses an EC<sub>50</sub> of 0.25 nM for inhibiting cellular mTOR activity. Compound 3 exhibited 800-fold selectivity over PI3K (EC<sub>50</sub>: 200 nM) and over 100-fold binding selectivity relative to 440 other protein kinases. Compound 3 has significantly improved bioavailability (54%), metabolic stability, and plasma exposure relative to compound 1.



## ■ INTRODUCTION

The mammalian target of rapamycin (mTOR) is a highly conserved serine/threonine protein kinase and is a key element in the PI3K/AKT/mTOR signal pathway.<sup>1</sup> Upon activation by extracellular inputs such as insulin, energy stress, growth factors, and nutrients, mTOR regulates a variety of fundamental cellular processes such as proliferation, growth, and metabolism.<sup>2,3</sup> mTOR is a member of PIKK kinase family, which also includes PI3K, ATR, ATM, DNA-PK, and SMG-1. Structurally their catalytic domains all share high sequence identity to the PI3K kinase but differ significantly in sequence and secondary structure from the protein kinases.<sup>4</sup> In cells mTOR exists in at least two functionally distinct protein complexes, mTORC1 and mTORC2. The mTORC1 complex is composed of Raptor, LST8, PRAS40, and Deptor and is responsible for regulated protein synthesis through phosphorylation of S6K1 and 4E-BP1. The mTORC2 complex consists of Rictor, LST8, SIN1, Deptor, and Protor and regulates cell proliferation and survival through phosphorylation of Akt/PKB.<sup>5</sup>

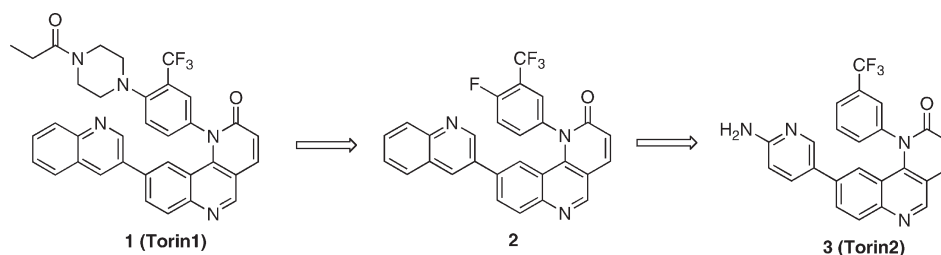
The PI3K/Akt/mTOR signal transduction pathway is frequently deregulated in human cancers and thereby has attracted considerable attention as an oncology drug discovery target.<sup>6–9</sup>

Successful development of rapalogues (rapamycin and related analogues) as treatments of specific cancers has provided clinical validation of mTOR as an anticancer drug discovery target.<sup>10</sup> However, existing rapalogues do not fully inhibit mTORC1 and are unable to acutely inhibit mTORC2.<sup>11,12</sup> In addition, a negative feedback loop exists through S6K/IRS1/PI3K that results in pathway activation upon inhibition of mTORC1 by rapamycin which may also serve to limit the efficacy of the rapalogues.<sup>13</sup> There is currently great interest in clinically testing the hypothesis that ATP-competitive mTOR inhibitors will exhibit more broad-based and profound antitumor activity relative to the rapalogues. In the recent years there has been a significant investment in developing potent and selective mTOR inhibitors which

Received: November 26, 2010

Published: February 15, 2011

## Scheme 1. Discovery of 3 Starting from 1

Table 1. Pharmacological Characterization of Compounds 1 and 2<sup>a</sup>

compd	mTORC1 IC <sub>50</sub> (nM)	mTOR EC <sub>50</sub> (nM)	PI3K EC <sub>50</sub> (nM)	mouse microsome stability, T <sub>1/2</sub> (min)
1	0.29	2	1800	4
2	37.1	25	>1250	17.7

<sup>a</sup> Determinations are the mean of two of independent measurements with standard error of <20%.

has resulted in compounds such as 2-(4-amino-1-isopropyl-1H-pyrazolo[3,4-d]pyrimidin-3-yl)-1H-indol-5-ol (PP242),<sup>14</sup> 5-(2-((2R,6S)-2,6-dimethylmorpholino)-4-morpholinopyrido[2,3-d]pyrimidin-7-yl)-2-methoxyphenylmethanol (KU63794),<sup>15</sup> 5-(2,4-bis-((S)-3-methylmorpholino)pyrido[2,3-d]pyrimidin-7-yl)-2-methoxyphenylmethanol (AZD8055),<sup>16</sup> methyl 4-(1-(1-(methoxycarbonyl)piperidin-4-yl)-4-morpholino-1H-pyrazolo[3,4-d]pyrimidin-6-yl)phenylcarbamate (WYE-354),<sup>17</sup> (1S,4S)-4-(4-amino-5-(7-methoxy-1H-indol-2-yl)imidazo[1,5-f][1,2,4]triazin-7-yl)cyclohexanecarboxylic acid (OSI-027),<sup>18</sup> 1-(4-(8-oxa-3-azabicyclo[3.2.1]octan-3-yl)-1-(1,4-dioxaspiro[4.5]decan-8-yl)-1H-pyrazolo[3,4-d]pyrimidin-6-yl)-3-methylurea (WYE-125132),<sup>19</sup> (E)-4-((2-(4,6-dimorpholino-1,3,5-triazin-2-yl)hydrazono)-methyl)-2,6-dimethoxyphenol (KU-BMCL-200908069-1),<sup>20</sup> 1-(4-(4-(8-oxa-3-aza-bicyclo[3.2.1]octan-3-yl)-1-(2,2,2-trifluoroethyl)-1H-pyrazolo[3,4-d]pyrimidin-6-yl)phenyl)-3-(4-(4-methylpiperazin-1-yl)phenyl)urea (Wyeth-BMCL-200910096-27),<sup>21</sup> and compound 1.<sup>22</sup>

Compound 1 is a highly potent and selective mTOR inhibitor that exhibits the ability to inhibit mTOR in vivo. However, the low yielding synthetic route, poor water solubility, short half-life (T<sub>1/2</sub>), and low oral bioavailability limits the use of 1 as a pharmacological tool in vivo. In order to address some of these deficiencies, we initiated a medicinal chemistry campaign that resulted in the identification of a highly potent and selective mTOR inhibitor 3 (Torin2), which is easier to produce on scale and exhibits improved pharmacokinetic properties that should enable its use in vivo.

## RESULTS AND DISCUSSION

Compound 1 exhibits very rapid metabolism upon incubation with mouse and human hepatocytes (T<sub>1/2</sub> of 4 min), which suggests that the compound may be subject to rapid first-pass metabolism in the liver. Consistent with this finding, the observed half-life following intravenous delivery of 1 to mice was 30 min. Oral administration of 1 revealed that the compound possessed very limited oral bioavailability. We

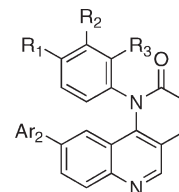


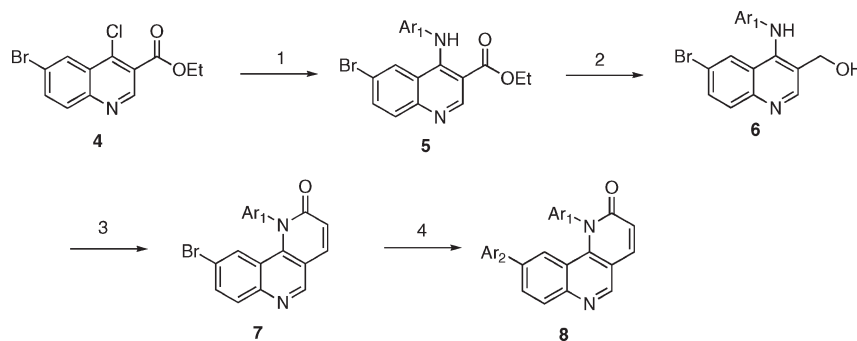
Figure 1. Representative structure of the library.

reasoned that if we could reduce the molecular weight of 1, we might remove sites of metabolism and also obtain a more water-soluble compound. Replacement of the propionylpiperazine moiety of 1 with a fluorine yielded compound 2 (Scheme 1) which maintained potent cellular mTOR (EC<sub>50</sub> = 25 nM) inhibitory activity and selectivity versus PI3K (EC<sub>50</sub> > 1250 nM). The isolated mouse microsome stability of compound was significantly improved compared to 1 (T<sub>1/2</sub> of 17.7 min) (Table 1). This result encouraged us to prepare a focused series of analogues with replacements to the quinoline moiety which ultimately resulted in the identification of 3 (Figure 1).

The targeted library was generated using a four-step synthetic sequence that commenced from 4-chloro-6-bromoquinoline compound 4 (Scheme 2). A nucleophilic substitution with appropriate anilines provided general intermediate 5, which was subsequently subjected to NaBH<sub>4</sub> reduction to afford the alcohol 6. Benzylic alcohol oxidation with MnO<sub>2</sub> followed by Horner–Wadsworth–Emmons olefination furnished the tricyclic core scaffold 7. Finally variation of the Ar<sub>2</sub> position was achieved using palladium mediated coupling reactions to afford the target compounds 8.

By variation the substitutions of the Ar<sub>1</sub> and Ar<sub>2</sub> groups, a focused library was generated (Figure 1) and the biological characterizations are summarized in Table 2.

Substitution of the acylpiperazine ring with fluoro at the R<sub>1</sub> position (compound 2) resulted in a 10-fold loss of potency in cellular mTOR assays. Replacement of the quinoline side chain at the Ar<sub>2</sub> position with pyrazole (9) and methylpyrazole (10) resulted in 5- to 25-fold reduction in activity. Replacement of the quinoline of 2 with aminopyridine (11), aminopyrimidine (12), and 7-azaindole (14) groups resulted in compounds with potent mTOR inhibitory activity. However, compounds 11 and related analogues demonstrated higher PI3K inhibitory activity. Indazole replacement (13) resulted in 10-fold loss of potency relative to 14, indicating that a β nitrogen was required for the activity, potentially suggesting a hydrogen-bond accepting moiety is required at this position. A similar activity trend was observed when CF<sub>3</sub> was substituted with CH<sub>3</sub> (15–21) at the R<sub>2</sub> position. 7-azaindole analogue (21) possessed the most

Scheme 2. Chemical Synthesis of a Focused Library<sup>a</sup>

<sup>a</sup> Reagents and conditions: (1) appropriate aniline, 1,4-dioxane, 90 °C, 4–12 h; (2) NaBH<sub>4</sub>, EtOH, room temp, 2–4 h; (3) (a) MnO<sub>2</sub>, CH<sub>2</sub>Cl<sub>2</sub>, room temp, 2–6 h; (b) triethyl phosphonoacetate, K<sub>2</sub>CO<sub>3</sub>, EtOH, 100 °C, 12 h; (4) Ar<sub>2</sub>B(OH)<sub>2</sub>, PdCl<sub>2</sub>(Ph<sub>3</sub>P)<sub>2</sub>, Na<sub>2</sub>CO<sub>3</sub>, 1,4-dioxane, 80 °C, 4–12 h.

potent mTOR inhibitory activity but also exhibited significant activity against PI3K. Replacement of CF<sub>3</sub> with smaller groups such as Cl (**22–26**) and F (**27, 28**) resulted in compounds with similar potency against mTOR and PI3K. 7-Azaindole analogue (**24**) and aminopyrimidine analogue (**25**) exhibited the best potency as inhibitors of mTOR while still possessing more than 500-fold selectivity relative to PI3K. Introduction of the CF<sub>3</sub> group at R<sub>3</sub> position (**29–31**) resulted in a 20- to 100-fold loss of activity against mTOR, suggesting either steric impediments to substitution at this position or unfavorable effects on the conformation of the compound. Removal of F from the R<sub>1</sub> position while maintaining the aminopyridine side chain (**3**) resulted in the best balance of highly potent inhibition of mTOR (EC<sub>50</sub> = 0.25 nM) while maintaining 800-fold selectivity relative to PI3K (EC<sub>50</sub> = 200 nM).

We attempted to rationalize the observed structure–activity relationship (SAR) by docking compound **3** into a homology model of mTOR built using a PI3Kγ crystal structure (PDB code 3DBS) (Figure 2A). Similar to **1**,<sup>22</sup> compound **3** is predicted to engage in a “hinge” hydrogen bond with Y2240 using the quinoline nitrogen as well as engage a second hydrogen bond between Y2225 and pyridine nitrogen inside inner hydrophobic pocket. In addition, two hydrogen bonds are predicted to exist between the aniline amino group of **3** with D2195 and D2357 in the inner hydrophobic pocket, and this may provide an explanation for the approximate 10-fold potency increase in mTOR inhibition compared to **1**. The same binding mode was observed in PI3Kγ modeling study with compound **3**. V882 served as a hinge binding point, and in the inner hydrophobic pocket Y867, D841 and D964 provided three more hydrogen bonds with aminopyridine side chain analogous to Y2225, D2195, and D2357 of mTOR. This may provide a rationale for why compound **3** begins to inhibit PI3K (Figure 2B).

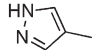
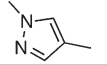
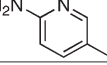
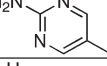
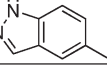
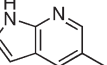
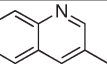
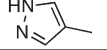
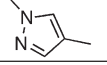
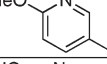
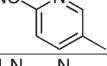
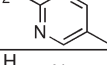
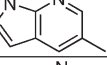
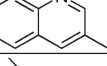
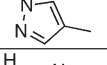
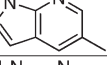
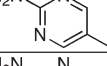
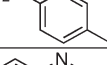
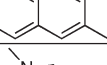
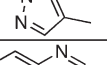
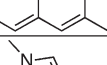
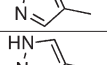
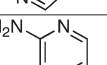

**Pharmacodynamics and Pharmacokinetics.** In order to determine which compounds might be optimal for use in murine tumor studies, we selected a set of compounds based on the mTOR activity, selectivity over PI3K, synthetic feasibility, and structural diversity. First the compounds were evaluated for their stability when incubated in the presence of isolated mouse liver microsomes. A subset of compounds were then advanced into pharmacodynamic (PD) studies monitoring the phosphorylation status of S6K T389 and Akt T308 in the lung and liver by Western blot 6 h after oral administration. The pharmacodynamic response was approximately scored with **1** being assigned a “+++” score (“++++” indicates over 95%, “+++” indicates

80–95%, “++” indicates 60–80%, and “+” indicates 40–60% inhibition of pS6K and pAkt compared to vehicle). The results are summarized in Table 3. Compounds **3**, **9**, **14**, **16**, and **17** exhibited similar or better pharmacodynamic effects relative to **1**, while compounds **2**, **15**, **23**, and **24** were less effective than **1**. Compounds **19**, **21**, **25**, **26**, **27**, and **28** did not exhibit inhibition of the S6K or Akt phosphorylation after 6 h. The liver microsome stability results varied significantly among the compounds. Compounds **2**, **3**, **19**, **25**, **26**, and **27** all exhibited more than a 10 min half-life, but this did not predict which compounds would exhibit a robust pharmacodynamic effect. Several compounds such as **19**, **25**, **26**, and **27** exhibited poor pharmacodynamics despite having superior microsome stability relative to **1**, while other very short-lived compounds such as **9**, **14**, **16**, and **17** exhibited more sustained pharmacodynamics. The basis for this discrepancy is currently unknown but may result from a sustained mTOR inhibition due to a slow off-rate from the kinase for some compounds. The oral PD studies employed a different formulation (10% NMP, 40% PEG in water) relative to the oral PK studies (0.5% w/v Na cmc with 0.1% w/v Tween-80), so the degree of drug exposure in the PD studies cannot be directly extrapolated from the PK studies.

Compounds that exhibited the best pharmacodynamic properties were subject to pharmacokinetic evaluation in mice following intravenous and oral administration (Table 4). As has been predicted by the mouse liver microsome stability study, all compounds exhibited a half-life of less than 2 h when dosed to male Swiss albino mice. Compound **3** exhibited the best bioavailability (51%) and overall exposure despite possessing a short half-life and was selected for further evaluation. Compared to compound **1**, the bioavailability of **3** was improved by approximately 10-fold.<sup>22</sup> Most of the compounds exhibited rapid absorption following oral administration to mice. All the compounds studied had low to moderate clearance and exhibited volumes of distribution close to the total body water. The possible reasons for the low bioavailability for the majority of the compounds could be poor absorption that may be due to the limited water solubility of the compounds.

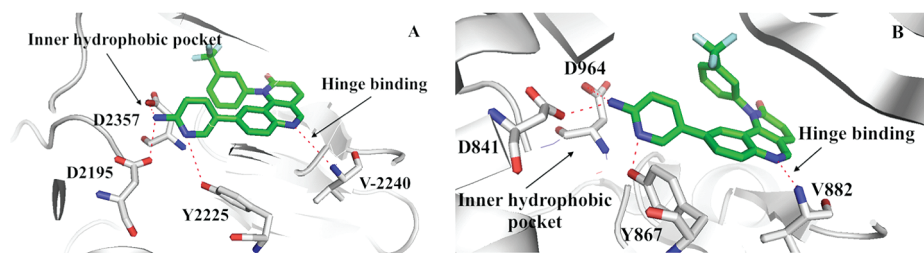
**Kinase Selectivity Profiling.** To characterize the kinase selectivity of **3**, we profiled its ability to bind to a panel of 440 kinases using the Ambit KinomeScan technology<sup>23</sup> (Table 5). Compound **3** exhibited excellent overall selectivity (S(5) score (1 μM) of 0.02)<sup>24</sup> and has strong binding to mTOR (4.6), CSNK1E (2.7), several PI3Ks (0–3.5), CSF1R (2.4), and MKNK2 (0.9). Compound **3** was subject to further profiling against a

Table 2. Enzymatic and Cellular Activities of Compounds 3 and 9–31<sup>a</sup>

Entry	R <sub>1</sub> (para)	R <sub>2</sub> (meta)	R <sub>3</sub> (ortho)	Ar <sub>2</sub>	mTORC1 IC <sub>50</sub> (nM)	mTOR EC <sub>50</sub> (nM)	PI3K EC <sub>50</sub> (nM)
9	F	CF <sub>3</sub>	H		4.6	10	>1250
10	F	CF <sub>3</sub>	H		69.3	50	1000
11	F	CF <sub>3</sub>	H		2.9	1	250
12	F	CF <sub>3</sub>	H		16.4	1	500
13	F	CF <sub>3</sub>	H		76.0	25	500
14	F	CF <sub>3</sub>	H		15.2	1	750
15	F	CH <sub>3</sub>	H		35.5	10	1000
16	F	CH <sub>3</sub>	H		7.0	10	>1250
17	F	CH <sub>3</sub>	H		59.5	50	1000
18	F	CH <sub>3</sub>	H		77.8	20	1000
19	F	CH <sub>3</sub>	H		303	20	>1250
20	F	CH <sub>3</sub>	H		43.0	10	>1250
21	F	CH <sub>3</sub>	H		2.2	2	250
22	F	Cl	H		26.7	10	500
23	F	Cl	H		79.2	50	1000
24	F	Cl	H		1.4	1	750
25	F	Cl	H		2.5	1	750
26	F	Cl	H		24.4	2	250
27	F	F	H		18.9	5	750
28	F	F	H		84.4	100	1000
29	F	H	CF <sub>3</sub>		4.8	25	>1250
30	F	H	CF <sub>3</sub>		107.5	250	1250
31	F	H	CF <sub>3</sub>		19.2	35	1250
3	H	CF <sub>3</sub>	H		2.1	0.25	200

<sup>a</sup>IC<sub>50</sub> determinations are the mean of two of independent measurement with standard error of <20%.





**Figure 2.** Model of **3** (green sticks) docked into a homology model of mTOR (gray ribbons) (A) and PI3K $\gamma$  (PDB code 3DBS) (gray ribbons) (B). Potential hydrogen bonds are shown with hatched red lines.

panel of lipid kinases using the Invitrogen SelectScreen technology which exhibited potent biochemical inhibition of PI3Ks and DNA-PK in addition to mTOR (Table 6). From our cellular PI3K assays we know there is approximately a 40-fold discrepancy between the biochemical PI3K IC<sub>50</sub> and the cellular EC<sub>50</sub>. It remains to be determined whether DNA-PK is inhibited by **3** in cellular assays. It is interesting to note that the enzymatic selectivity ratio for inhibition of mTOR versus PI3K for both **3** (enzyme ratio of 2) and Torin1 (enzyme ratio of 60)<sup>22</sup> substantially underestimates the observed ratio for cellular inhibition of these targets: **3** (cell ratio of 800) and Torin1 (cell ratio of 900).

## CONCLUSION

Starting from the selective mTOR inhibitor **1**, we used a focused medicinal chemistry approach guided by cellular assays and pharmacokinetic and pharmacodynamic assays to develop **3** which possesses properties that make it more suitable for use in murine tumor studies. Compound **3** possesses a 250 pM EC<sub>50</sub> for inhibiting mTOR in cells while maintaining 800-fold cellular selectivity relative to inhibition of PI3K and most other protein kinases. Compound **3** exhibits good bioavailability and exposure and can maintain strong inhibition of mTOR activity in lung and liver to at least 6 h after a single dose of 20 mg/kg. Compound **3** is a useful pharmacological tool for further exploring the therapeutic potential of mTOR inhibitors for the treatment of cancer.

## EXPERIMENTAL PROCEDURES

**Chemistry.** All solvents and reagents were used as obtained. <sup>1</sup>H NMR spectra were recorded with a Varian Inova 600 NMR spectrometer and referenced to dimethylsulfoxide. Chemical shifts are expressed in ppm. In the NMR tabulation, s indicates singlet; d, doublet; t, triplet; q, quartet; m, multiplet; and br, broad peak. Mass spectra were measured with Waters Micromass ZQ using an ESI source coupled to a Waters 2525 HPLC system operating in reverse mode with a Waters Sunfire C18 5  $\mu$ m, 4.6 mm  $\times$  50 mm column. Purification of compounds was performed with either a Teledyne ISCO CombiFlash Rf system or a Waters Micromass ZQ preparative system. The purity of all compounds was  $\geq$ 95%. The purity was analyzed on an above-mentioned Waters LC–MS Symmetry (C18 column, 4.6 mm  $\times$  50 mm, 5  $\mu$ m) using a gradient of 5–95% acetonitrile in water containing 0.05% trifluoroacetic acid (TFA) over 8 min (10 min run time) at a flow rate of 2 mL/min.

**General Procedure for the Preparation of Compounds.** To a solution of compound **4** (ethyl 6-bromo-4-chloroquinoline-3-carboxylate, 1 equiv) in 1,4-dioxane at room temperature in a sealed tube was added aniline (1 equiv). The resultant solution was heated

to 90 °C for 4–12 h. After the mixture was cooled to room temperature, a solution of NaOH (1 N) was added to neutralize the solution followed by dilution with water and extraction with ethyl acetate. After the mixture was dried with Na<sub>2</sub>SO<sub>4</sub>, the solvents were removed and the residue was purified by ISCO (hexanes/EtOAc) to furnish compound **5**.

To a solution of compound **5** (1 equiv) in EtOH at room temperature was added NaBH<sub>4</sub> (10 equiv). The resultant solution was stirred at room temperature for 2–4 h before being diluted with EtOAc and filtered through Celite. The filtrate was concentrated under vacuum, and the residue was dissolved in EtOAc and brine. After separation, the organic layer was dried over MgSO<sub>4</sub> and concentrated under vacuum. The residue was purified by ISCO (hexanes/EtOAc) to afford compound **6**.

To a solution of compound **6** in CH<sub>2</sub>Cl<sub>2</sub> (1 equiv) at room temperature was added MnO<sub>2</sub> (5 equiv mass). After 2–6 h, the reaction mixture was filtered through Celite. The filtrate was concentrated in a sealed tube and dissolved in dry EtOH, after which K<sub>2</sub>CO<sub>3</sub> (3 equiv) and triethyl phosphonoacetate were added. The resulting mixture was heated to 100 °C for 12 h before cooling to room temperature. Upon removal of the solvents under vacuum, the residue was diluted with water followed by extraction with EtOAc. Purification of the residue by ISCO (hexanes/EtOAc) provided compound **7**.

To a solution of compound **7** in 1,4-dioxane at room temperature was subsequently added PdCl<sub>2</sub>(Ph<sub>3</sub>P)<sub>2</sub> (0.1 equiv), Na<sub>2</sub>CO<sub>3</sub> (3 equiv, 1 N), and boronic acids or pinacol boronate esters. After degassing, the resulting mixture was heated to 80 °C for 4–12 h before cooling to room temperature and filtering through Celite. Upon removal of the solvents, the residue was subjected to column purification (CH<sub>2</sub>Cl<sub>2</sub>/MeOH) to furnish the desired compounds **8**.

Compound **3** was prepared following the above procedures (15% overall yield). LC–MS: (M + H) 433.13. <sup>1</sup>H NMR (600 MHz, DMSO-*d*<sub>6</sub>)  $\delta$  9.09 (s, 1H), 8.31 (d, *J* = 9.6 Hz, 1H), 8.11 (s, 1H), 8.03 (d, *J* = 9.0 Hz, 1H), 8.00 (d, *J* = 7.8 Hz, 1H), 7.92 (dd, *J* = 8.4, 1.8 Hz, 1H), 7.86 (dd, *J* = 8.4, 7.8 Hz, 1H), 7.78 (d, *J* = 8.4 Hz, 1H), 7.72 (d, *J* = 2.4 Hz, 1H), 7.04 (dd, *J* = 8.4, 2.4 Hz, 1H), 6.91–6.93 (m, 2H), 6.38 (d, *J* = 8.4 Hz, 1H), 6.18 (s, 2H).

For characterization of *in vitro* biochemical activity with the mTORC1 complex, mTOR and PI3K cellular assays, Ambit *in vitro* KinomeScan kinase selectivity profile, and *in vivo* pharmacokinetic studies, see ref 22.

**In Vivo Pharmacodynamic Studies.** Compound **3** powder was first dissolved at 25 mg/mL in 100% *N*-methyl-2-pyrrolidone and then diluted 1:4 with sterile 50% PEG400 prior to injection. Six-week-old male C57BL/6 mice were fasted overnight prior to drug treatment. The mice were treated with vehicle (for 10 h) or **3** (20 mg/kg for 6 h) via oral gavage and then refed 1 h prior to sacrifice (CO<sub>2</sub> asphyxiation). Liver and lung were collected and frozen on dry ice. The frozen tissue was thawed on ice and lysed by sonication in tissue lysis buffer (50 mM HEPES, pH 7.4, 40 mM NaCl, 2 mM EDTA, 1.5 mM sodium orthovanadate, 50 mM sodium fluoride, 10 mM sodium pyrophosphate,

Table 3. Pharmacodynamics and Liver Microsome Stability of Selected Compounds

Entry	Structure	PD	T <sub>1/2</sub> (min)	PI3K/mTOR (Selectivity fold)
2		++	11.7	50
3		+++++	11.7	800
9		+++	4.2	125
14		+++++	1.5	750
15		++	3.3	100
16		+++++	3.2	83
17		+++++	2.7	20
19		None	14.4	62.5
21		None	1.8	125
23		++	3.7	20
24		++	2.1	750
25		None	20.6	750
26		None	14.5	500
27		None	22.9	150
28		None	4.5	10

Table 4. PK Properties of Selected Compounds<sup>a</sup>

compd	C <sub>max</sub> (ng/mL) iv/po	T <sub>max</sub> (h) po	AUC (h·ng/mL) iv/po	T <sub>1/2</sub> (h) iv	CL ((mL/min)/kg) iv	V <sub>ss</sub> (L/kg) iv	F (%) po
3	1540/3968	0.25	850/4311	0.72	19.6	1.0	51
9	426/430	0.5	391/755	0.63	42.6	2.42	19.2
14	1639/98	1.0	803/352	1.09	20.8	1.30	4.2
16	1035/853	0.5	1110/2410	1.46	15.0	1.16	21.6
17	—/1039	0.5	728/2068	0.99/1.31	22.9	1.08	28

<sup>a</sup> C57BL/6 male mouse was dosed at 1 mg/kg for the intravenous (iv) and at 10 mg/kg for the oral (po).

Table 5. Kinome Scan Profile of 3<sup>a</sup>

kinase	% control	kinase	% control
mTOR	4.6	CSF1R	2.4
CSNK1E	2.7	MKNK2	0.9
PIK3C2G	3.5	PIK3CA	0.55
PIK3CA(C420R)	0.1	PIK3CA(E542K)	0.25
PIK3CA(E545K)	0.25	PIK3CA(H1047L)	0
PIK3CA(H1047Y)	1.4	PIK3CA(I800L)	0
PIK3CA(M1043I)	1	PIK3CA(Q546K)	0.35
PIK3CG	0.2	PIK4CB	1.7

<sup>a</sup> Compound 3 was profiled at 1  $\mu$ M against a diverse panel of 442 kinases by Ambit Biosciences.

Table 6. LanthaScreen Profile of 3 Using the Invitrogen Lipid Kinase Panel<sup>a</sup>

kinase	IC <sub>50</sub> (nM)	kinase	IC <sub>50</sub> (nM)
PI4K $\alpha$	>10000	P110 $\alpha$ /p85 $\alpha$	4.68
PI4K $\beta$	18.3	P110 $\delta$ /P85 $\alpha$	17.5
PI3K-C2 $\alpha$	28.1	P110 $\gamma$	5.67
PI3K-C2 $\beta$	24.5	DNA-PK	0.5
hVPS34	8.58	mTOR	2.81

<sup>a</sup> Kinase targets were tested with biochemical enzymatic kinase assays using the SelectScreen Kinase Profiling Service (Life Technologies Corporation, Madison, WI).

10 mM sodium  $\beta$ -glycerophosphate, 0.1% SDS, 1.0% sodium deoxycholate, and 1.0% Triton, supplemented with protease inhibitor cocktail tablets (Roche)). The concentration of clear lysate was measured using the Bradford assay, and samples were subsequently normalized by protein content and analyzed by SDS-PAGE and immunoblotting.

**Molecular Modeling.** Compound 3 was docked into an mTOR homology model built from a published PI3K $\gamma$  crystal structure complexed with GDC-0941 (PDB code 3DBS) using AutoDock vina.<sup>22,25</sup>

## ■ ASSOCIATED CONTENT

**S Supporting Information.** Spectral data of 2 and 9–31. This material is available free of charge via the Internet at <http://pubs.acs.org>.

## ■ AUTHOR INFORMATION

### Corresponding Author

\*Phone: 1-617-582-8590. Fax: 1-617-582-8615. E-mail: [Nathanael\\_gray@dfci.harvard.edu](mailto:Nathanael_gray@dfci.harvard.edu).

## ■ ACKNOWLEDGMENT

We thank Life Technologies Corporation, SelectScreen Kinase Profiling Service for performing enzymatic biochemical kinase profiling, and Ambit Bioscience for performing KinomeScan profiling. We also want to thank Sai Advantium Pharma Ltd. (India) for the pharmacokinetic studies and Michael Cameron for performing in vitro microsome stability studies. This work was partially supported by NIH Grant GM079575-03.

## ■ ABBREVIATIONS USED

mTOR, mammalian target of rapamycin; Akt, v-akt murine thymoma viral oncogene homologue 1; ATP, adenosine triphosphate; PIKK, PI3K related kinases; DNA-PK, DNA activated protein kinase; ATM, ataxia telangiectasia mutated kinase; ATR, ataxia telangiectasia and Rad-3-related kinase; SMG-1, serine/threonine protein kinase -1; 4E-BP1, eukaryotic translation initiation factor 4E-binding protein 1; PK, pharmacokinetics

## ■ REFERENCES

- (1) Guertin, D. A.; Sabatini, D. M. Defining the role of mTOR in cancer. *Cancer Cell* **2007**, *12*, 9–22.
- (2) Sarbassov, D. D.; Ali, S. M.; Sabatini, D. M. Growing roles for the mTOR pathway. *Curr. Opin. Cell. Biol.* **2005**, *17*, 596–603.
- (3) Ma, X. M.; Blenis, J. Molecular mechanisms of mTOR mediated translational control. *Nat. Rev. Mol. Cell Biol.* **2009**, *10*, 307–318.
- (4) Abraham, R. T. PI 3-kinase related kinases: “big” players in stress-induced signaling pathways. *DNA Repair* **2004**, *3*, 883–887.
- (5) Sabatini, D. M. mTOR and cancer: insights into a complex relationship. *Nat. Rev. Cancer* **2006**, *6*, 729–734.
- (6) Shaw, R. J.; Cantley, L. C. Ras, PI(3)K and mTOR signaling controls tumour cell growth. *Nature* **2006**, *441*, 424–430.
- (7) Faivre, S.; Kroemer, G.; Raymond, E. Current development of mTOR inhibitors as anticancer agents. *Nat. Rev. Drug Discovery* **2006**, *5*, 671–688.
- (8) Shor, B.; Gibbons, J. J.; Abraham, R. T.; Yu, K. Targeting mTOR globally in cancer: thinking beyond rapamycin. *Cell Cycle* **2009**, *8*, 3831–3837.
- (9) Meric-Bernstam, F.; Gonzalez-Angulo, A. M. Targeting the mTOR signaling network for cancer therapy. *J. Clin. Oncol.* **2009**, *27*, 2278–2287.
- (10) Lane, H. A.; Breuleux, M. Optimal targeting of the mTORC1 kinase in human cancer. *Curr. Opin. Cell Biol.* **2009**, *21*, 219–229.
- (11) Thoreen, C. C.; Kang, S. A.; Chang, J.; Liu, Q.; Zhang, J.; Gao, Y.; Reichling, L. J.; Sim, T.; Sabatini, D. M.; Gray, N. S. An ATP-competitive mammalian target of rapamycin inhibitor reveals rapamycin-resistant functions of mTORC1. *J. Biol. Chem.* **2009**, *284*, 8023–8032.
- (12) Jacinto, E.; Loewith, R.; Schmidt, A.; Lin, S.; Ruegg, M. A.; Hall, A.; Hall, M. N. Mammalian TOR complex2 controls the actin cytoskeleton and is rapamycin insensitive. *Nat. Cell Biol.* **2004**, *6*, 1122–1128.
- (13) Wan, X.; Harkavy, B.; Shen, N.; Grohar, P.; Helman, L. J. Rapamycin induces feedback activation of Akt signaling through an IGF-1R-dependent mechanisms. *Oncogene* **2007**, *26*, 1932–1940.

(14) Feldman, M. E.; Apse, B.; Uotila, A.; Loewith, R.; Knight, Z. A.; Ruggero, D.; Shokat, K. M. Active-site inhibitors of mTOR target rapamycin-resistant outputs of mTORC1 and mTORC2. *PLoS Biol.* **2009**, *7*, 371–383.

(15) Garcia-Martinez, J. M.; Moran, J.; Clarke, R. G.; Gray, A.; Cosulich, S. C.; Chresta, C. M.; Alessi, D. R. Ku-0063794 is a specific inhibitor of the mammalian target of rapamycin (mTOR). *Biochem. J.* **2009**, *421*, 29–42.

(16) Chresta, C. M.; Davies, B. R.; Hickson, I.; Harding, T.; Cosulich, S.; Critchlow, S. E.; Vincent, J. P.; Ellson, R.; Jones, D.; Sini, P.; James, D.; Howard, Z.; Dudley, P.; Hughes, G.; Smith, L.; Maguire, S.; Hummersone, M.; Malagu, K.; Menear, K.; Jenkins, R.; Jacobsen, M.; Smith, G. C. M.; Guichard, S.; Pass, M. AZD8055 is a potent, selective, and orally bioavailable ATP-competitive mammalian target of rapamycin kinase inhibitor with in vitro and in vivo antitumor activity. *Cancer Res.* **2010**, *70*, 288–298.

(17) Yu, K.; Toral-Barza, L.; Shi, C.; Zhang, W.; Lucas, J.; Shor, B.; Kim, J.; Verheijen, J.; Curran, K.; Malwitz, D. J.; Cole, D. C.; Ellingboe, J.; Ayril-kaloustian, S.; Mansour, T. S.; Gibbons, J. J.; Abraham, R. T.; Nowak, P.; Zask, A. Biochemical, cellular, and in vivo activity of novel ATP-competitive and selective inhibitors of the mammalian target of rapamycin. *Cancer Res.* **2009**, *69*, 6232–6240.

(18) Barr, S.; Russo, S.; Buck, E.; Epstein, D.; Miglarese, M. Co-Targeting mTOR and IGF-1R/IR Results in Synergistic Activity against a Broad Array of Tumor Cell Lines, Independent of KRAS Mutation Status. Presented at the 101st Annual Meeting of the AACR, Washington DC, April, 2010; 1632.

(19) Yu, K.; Shi, C.; Toral-Barza, L.; Shor, B.; Kim, J. E.; Zhang, W. G.; Mahoney, R.; Gaydos, C.; Tardio, L.; Kim, S. K.; Conant, R.; Curran, K.; Kaplan, J.; Verheijen, J.; Ayril-kaloustian, S.; Mansour, T. S.; Abraham, R. T.; Zask, A.; Gibbons, J. J. Beyond rapalog therapy: preclinical pharmacology and antitumor activity of WYE-125132, an ATP-competitive and specific inhibitor of mTORC1 and mTORC2. *Cancer Res.* **2010**, *70*, 621–631.

(20) Menear, K. A.; Gomez, S.; Malagu, K.; Balley, C.; Blackburn, K.; Cockcroft, X.; Ewen, S.; Fundo, A.; Gall, A. L.; Hermann, G.; Sebastian, L.; Sunose, M.; Persnot, T.; Torode, E.; Hickson, I.; Martin, N. M.; Smith, G. C. M.; Pike, K. G. Identification and optimization of novel and selective small molecular weight kinase inhibitors of mTOR. *Bioorg. Med. Chem. Lett.* **2009**, *19*, 5898–5901.

(21) Richard, D. J.; Verheijen, J. C.; Curran, K.; Kaplan, J.; Troal-Barza, L.; Hollander, L.; Lucas, J.; Yu, K.; Zask, A. Incorporation of water-solubilizing groups in pyrazolopyrimidine mTOR inhibitors: discovery of highly potent and selective analogs with improved human microsomal stability. *Bioorg. Med. Chem. Lett.* **2009**, *19*, 6830–6835.

(22) Liu, Q.; Chang, J.; Wang, J.; Kang, S. A.; Thoreen, C. C.; Markhard, A.; Hur, W.; Zhang, J.; Sim, T.; Sabatini, D. M.; Gray, N. S. Discovery of 1-(4-(4-propionylpiperazin-1-yl)-3-(trifluoromethyl)-phenyl)-9-(quinolin-3-yl)benzo[h][1,6]naphthyridin-2(1H)-one as a highly potent, selective mammalian target of rapamycin (mTOR) inhibitor for the treatment of cancer. *J. Med. Chem.* **2010**, *53*, 7146–7155.

(23) Fabian, M. A.; Biggs, W. H., III; Treiber, D. K.; Atteridge, C. E.; Azimioara, M. D.; Benedetti, M. G.; Carter, T. A.; Ciceri, P.; Edeen, P. T.; Floyd, M.; Ford, J. M.; Galvin, M.; Gerlach, J. L.; Grotzfeld, R. M.; Herrgard, S.; Insko, D. E.; Insko, M. A.; Lai, A. G.; Lélis, J. M.; Mehta, S. A.; Milanov, Z. V.; Velasco, A. M.; Wodicka, L. M.; Patel, H. K.; Zarrinkar, P. P.; Lockhart, D. J. A small molecule-kinase interaction map for clinical kinase inhibitors. *Nat. Biotechnol.* **2005**, *23*, 329–336.

(24) For selectivity score calculation  $S(5)$ , see [http://www.kinomesan.com/pdfs/Screening\\_Report\\_New.pdf](http://www.kinomesan.com/pdfs/Screening_Report_New.pdf).

(25) Trott, O.; Olson, A. J. Autodock Vina: improving the speed and accuracy of docking with a new scoring function, efficient optimization, and multithreading. *J. Comput. Chem.* **2010**, *31*, 455–461.